



# Effect of $\text{Al}_2\text{O}_3$ – $\text{SiO}_2$ Composites on the Breakdown Voltage and Physicochemical Properties of Palm-Based Transformer Oil

Athala Kevin B.G. Maturbongs<sup>1</sup>, Zainal Alim Mas'ud<sup>1</sup>, Mohammad Khotib<sup>1,\*</sup>,  
 Roza Indra Laksmana<sup>2</sup>

<sup>1</sup> Department of Chemistry, Faculty of Mathematics and Natural Sciences, IPB University, Bogor, Indonesia

<sup>2</sup> National Research and Innovation Agency (BRIN), Tangerang Selatan, Indonesia

\* Corresponding author: [mohammadkh@apps.ipb.ac.id](mailto:mohammadkh@apps.ipb.ac.id)

<https://doi.org/10.14710/jksa.28.9.471-480>

## Article Info

### Article history:

Received: 12<sup>th</sup> June 2025

Revised: 03<sup>rd</sup> November 2025

Accepted: 10<sup>th</sup> November 2025

Online: 8<sup>th</sup> December 2025

### Keywords:

$\text{Al}_2\text{O}_3$ – $\text{SiO}_2$  composite; dielectric properties; palm oil; sol–gel synthesis; transformer oil

## Abstract

Mineral oil is a type of transformer oil commonly used as a coolant and electrical insulator, playing a vital role in transformer performance. However, its low biodegradability and environmental toxicity have prompted research into alternative materials. Palm oil has emerged as a promising substitute due to its biodegradability, favorable electrical properties, and abundance. This study aims to evaluate the effect of  $\text{Al}_2\text{O}_3$ – $\text{SiO}_2$  particles on the breakdown voltage (BDV) of palm oil as transformer oil. The particles were synthesized using the sol–gel method and characterized by FTIR, XRD, PSA, and SEM. They were then dispersed into palm oil at a concentration of 0.5 g/L. The BDV performance of  $\text{Al}_2\text{O}_3$ – $\text{SiO}_2$  was compared with that of single-component particles ( $\text{Al}_2\text{O}_3$  and  $\text{SiO}_2$ ) to assess their differences. In addition to BDV, other parameters—including color scale, total acid number, density, kinematic viscosity, and functional groups—were analyzed and compared to the quality standards specified in ASTM D6871-17 and IEC 62270:2018. The results showed that  $\text{Al}_2\text{O}_3$ – $\text{SiO}_2$  particles yielded higher BDV, moisture content, density, and viscosity, but a lower acid number in palm oil compared to single-component particles. Overall, palm oil with dispersed particles met the required quality standards for use as transformer oil.

## 1. Introduction

Transformer oil functions both as a cooling medium and an electrical insulator, making it crucial to transformer lifespan [1]. The type of transformer oil commonly used is mineral oil. Even though it is often used as transformer oil, mineral oil is non-renewable, with low biodegradability, and is toxic to the environment [2]. These aspects are leading to the need to find a substitute for mineral oil as transformer oil [1, 3].

An alternative to transformer oil that has been widely researched for its potential is vegetable oil (VO). VOs are obtained by extracting seeds, flowers, or fruits [4, 5]. Compared to mineral oil, VO is non-toxic with high biodegradability. Even though it is superior in several parameters compared to mineral oil, VO also has disadvantages, including the high content of unsaturated fatty acids, which makes the oil more susceptible to oxidation [4].

Thus, in order to improve the properties of VO, modifications are needed. One type of modification that can be applied is by adding filler to the VO. Single particle fillers such as  $\text{TiO}_2$ , ZnO,  $\text{SiO}_2$ ,  $\text{Al}_2\text{O}_3$ , and  $\text{Fe}_3\text{O}_4$  have been used and reported to improve the electrical properties of transformer oil [6]. Fillers can be added by synthesizing and dispersing the fillers in the VO simultaneously or by preparing the fillers first, followed by dispersing them in the VO [7].

The addition of fillers has been reported to improve the dielectric and physicochemical properties of VO. Saenkhumwong and Suksri [8] conducted research to compare the effects of ZnO and  $\text{TiO}_2$  fillers at various concentrations on the dielectric properties of palm ester. The research resulted in the breakdown voltage (BDV) of palm ester increasing as the concentration of  $\text{TiO}_2$  (between 7% and 54%) and ZnO (between 6% and 44%) increased. Khaled and Beroual [9] also reported the BDV

increment by 28 to 109% on natural ester oil-based nanofluid with various concentrations of  $\text{Fe}_3\text{O}_4$ .

Alumina ( $\text{Al}_2\text{O}_3$ ) is a common filler used in transformer oil to improve the thermal and electrical properties [10]. Nevertheless, high dielectric constant ( $\kappa$ ) material, such as alumina, presents some disadvantages, aggravated by lower thermal stability compared to conventional dielectrics such as  $\text{SiO}_2$  [11]. The electrical properties of insulating materials are correlated to their thermal stability. A low or decreased thermal stability of insulating material will lead to the deterioration of its electrical properties [12]. To improve the thermal stability of alumina, the incorporation of a suitable dopant is needed.  $\text{SiO}_2$  can be used as a dopant to enhance the thermal stability of alumina [13]. While having a relatively low permittivity ( $\epsilon_r = 3.9$ ),  $\text{SiO}_2$  is stable, has a very high band gap ( $E_g$ ) of 9 eV, and has a low defect density, making it a good insulator with a high breakdown voltage [11]. Therefore, this research was conducted to synthesize hybrid  $\text{Al}_2\text{O}_3$ - $\text{SiO}_2$  particles by sol-gel method and to observe their effects on physicochemical properties and BDV improvement compared to their single form as fillers for palm-based transformer oils.

## 2. Experimental

### 2.1. Materials

The materials used in this research were palm oil, distilled water,  $\text{AlCl}_3 \cdot 6\text{H}_2\text{O}$  (Pudak Scientific), tetraethyl orthosilicate (TEOS) (Merck), HCl (Merck, 37%), NaOH pellets (Merck), ethanol (Merck, 96%), phenolphthalein indicator, *p*-naphtholbenzein indicator, KOH pellets (Merck),  $\text{Ba}(\text{OH})_2$  (Merck), isopropyl alcohol (Merck), toluene (Merck), and potassium hydrogen phthalate (Merck).

### 2.2. Particle Synthesis

Particle synthesis was referred to as the research of Wu *et al.* [14] and Tian *et al.* [15] with a slight modification.  $\text{AlCl}_3 \cdot 6\text{H}_2\text{O}$  and TEOS were dissolved in 200 mL of ethanol solution (7:3) and homogenized. The total amount of  $\text{AlCl}_3 \cdot 6\text{H}_2\text{O}$  and TEOS was 0.2 mol. The samples were labelled according to the molar ratios of  $\text{AlCl}_3 \cdot 6\text{H}_2\text{O}$ : TEOS as  $\text{Al}_2\text{O}_3$  (1:0),  $\text{SiO}_2$  (0:1), and  $\text{Al}_2\text{O}_3$ - $\text{SiO}_2$  (1:1). The formed solution was then added with HCl until the pH of the solution reached 2. Once the solution was homogeneous, the solution was neutralized with NaOH (pH = 7) and left overnight. After that, the sample was centrifuged at 5000 rpm for 15 minutes to obtain a solid sample. The solid sample was then dried overnight at 105°C and then cooled to be ground. The process ended with calcination at 600°C for 2 hours.

### 2.3. Particle Characterizations

The synthesized particles were characterized by their morphologies using Scanning Electron Microscope (SEM) Hitachi SU3500, crystalline phases using X-ray Diffraction (XRD) Bruker D8 Advance with  $2\theta$  range of 5–90°, particle size using Particle Size Analyzer (PSA) Nanoplus Particulate Systems, and functional groups using Fourier Transform Infrared (FTIR) Shimadzu IRPrestige-21.

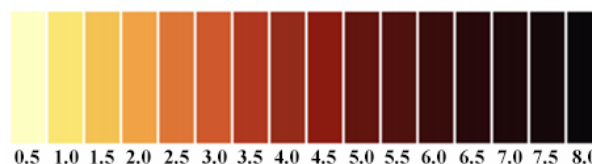


Figure 1. Color chart of transformer oil based on ASTM D1500 standard [16]

### 2.4. Synthesis of Palm-Based Transformer Oil

Synthesis of transformer oil was referred to Raj *et al.* [17] with a slight modification. Transformer oils were synthesized by dispersing  $\text{Al}_2\text{O}_3$ ,  $\text{SiO}_2$ , and  $\text{Al}_2\text{O}_3$ - $\text{SiO}_2$  into palm oil with a concentration of 0.5 g/L, and then were heated at 105°C for 12 hours. The synthesized transformer oils were cooled and then sonicated at 30 kHz for 2 hours [18, 19].

### 2.5. Determination of Oil Color Scale

Color analysis of transformer oil was conducted based on the ASTM D1524–15 standard method by visually observing the oil's appearance. The color was then matched to the ASTM D1500 color scale, where a color scale value of  $\leq 1$  indicates a bright, clear oil with no visible sediment. The color index results are shown in Figure 1.

### 2.6. Determination of Oil Moisture Content

Determination of moisture content followed the SNI 7431:2022 standard method. The petri dish was heated in the oven at 105°C for  $\pm 3$  hours and placed in a desiccator for  $\pm 30$  minutes, then the petri dish was weighed to get the initial weight of the petri dish ( $W_0$ ). Next, 5 grams of the oil sample was added to the petri dish and weighed ( $W_1$ ). The petri dish was heated in the oven at 105°C for  $\pm 3$  hours. Next, the petri dish was placed in a desiccator for  $\pm 30$  minutes and then weighed ( $W_2$ ). The test was repeated in three replicates. The water content of oil was calculated using Equation (1).

$$\text{Moisture content (\%)} = \frac{W_1 - W_2}{W_1 - W_0} \times 100\% \quad (1)$$

### 2.7. Determination of Oil Acid Number

Determination of the acid number in transformer oil followed the ASTM D974–21 standard method. 2 grams of oil were weighed, then 10 mL of titration solution (the solution was made by mixing toluene, distilled water, and isopropyl alcohol in a ratio of 100:1:99) was added, and 3 drops of *p*-naphtholbenzein indicator were added. Titration was carried out by using alcoholic KOH 0.1 M, and the color changes from orange to brownish green. The blank titration was carried out with 10 mL of titration solution, and 3 drops of *p*-naphtholbenzein were added. The blank was then titrated with alcoholic KOH 0.1 M, and color changes from orange to brownish green. Then the acid number was calculated, and the test was done in three replicates. The acid number was calculated using Equation (2).

$$\text{Total acid number} \left( \frac{\text{mg KOH}}{\text{g}} \right) = \frac{(A-B)M \times 56.1}{W} \quad (2)$$

Where, A is the KOH required for sample titration, B is the KOH required for blank titration, M is the molarity of KOH, and W is the sample weight.

## 2.8. Determination of Oil BDV and Dielectric Enhancement

Determination of BDV followed the IEC 60156:2018 standard method using the HZJQ-1B Transformer Oil BDV Tester. The gap between the mushroom-shaped electrodes was set to 2.5 mm. The sample was homogenized before being transferred into the oil chamber. A total of 300 mL of the oil sample was introduced into the chamber at room temperature, which served as the test temperature. The electrode was then applied with a constant voltage rate of rise at 2.0 kV/s until the breakdown voltage occurred. The test was carried out by continuous stirring with a standing time of 15 minutes, a pause time of 5 minutes, and a total test number of 6. The dielectric enhancement was calculated using Equation (3) [20].

$$\text{Enhancement (\%)} = \left( \frac{\text{BDV of transformer oil formula}}{\text{BDV of base transformer oil}} - 1 \right) \times 100 \quad (3)$$

## 2.9. Determination of Oil Density

Determination of density in transformer oil followed the SNI 7182:2015 standard method. The empty pycnometer was weighed. The oil was set at 20°C and then put into the pycnometer. The pycnometer was weighed again, and the test was repeated in three replicates. Density was measured using Equation (4).

$$\rho = \frac{(\text{pycnometer} + \text{sample}) - \text{empty pycnometer}}{\text{sample volume}} \quad (4)$$

## 2.10. Determination of Oil Viscosity

Determination of density refers to research by Amelia and Akhyan [21] with a slight modification using a Brookfield viscometer (Ametek DVPlus). The sample was heated at a temperature of 40°C, then the viscosity was tested with an LV-2(62) spindle at a rotation speed of 100 rpm. The value obtained was in the form of dynamic viscosity. The obtained dynamic viscosity was then converted into kinematic viscosity. Dynamic viscosity was obtained from the relationship between kinematic viscosity and density using Equation (5).

$$\mu = v \times \rho \quad (5)$$

The kinematic viscosity was obtained through Equation (6).

$$v = \frac{\mu}{\rho} \quad (6)$$

Where,  $\mu$  is the dynamic viscosity (cP or mPa·s),  $v$  is the kinematic viscosity (cSt or mm<sup>2</sup>/s), and  $\rho$  is the density (g/cm<sup>3</sup>).

## 3. Results and Discussion

### 3.1. Physical and Chemical Characteristics of The Synthesized Particles

#### 3.1.1. Physical Appearance of Synthesized Particles

Synthesis of three types of particles was conducted, namely SiO<sub>2</sub>, Al<sub>2</sub>O<sub>3</sub>, and hybrid Al<sub>2</sub>O<sub>3</sub>-SiO<sub>2</sub>. The synthesized samples were all in the form of white powder (Figure 2). The synthesized samples were then further analyzed for their phases, morphologies, and functional groups.

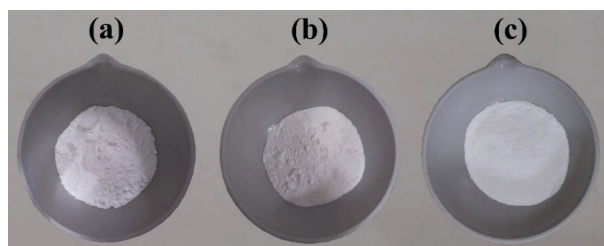


Figure 2. Physical appearance of (a) SiO<sub>2</sub>, (b) Al<sub>2</sub>O<sub>3</sub>, and (c) Al<sub>2</sub>O<sub>3</sub>-SiO<sub>2</sub>

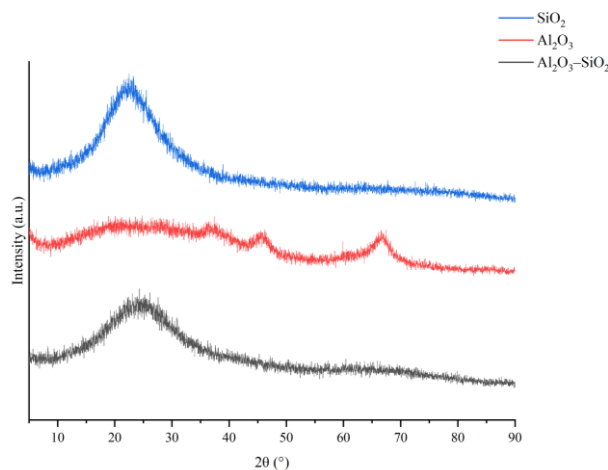


Figure 3. XRD diffractogram of SiO<sub>2</sub>, Al<sub>2</sub>O<sub>3</sub>, and Al<sub>2</sub>O<sub>3</sub>-SiO<sub>2</sub>

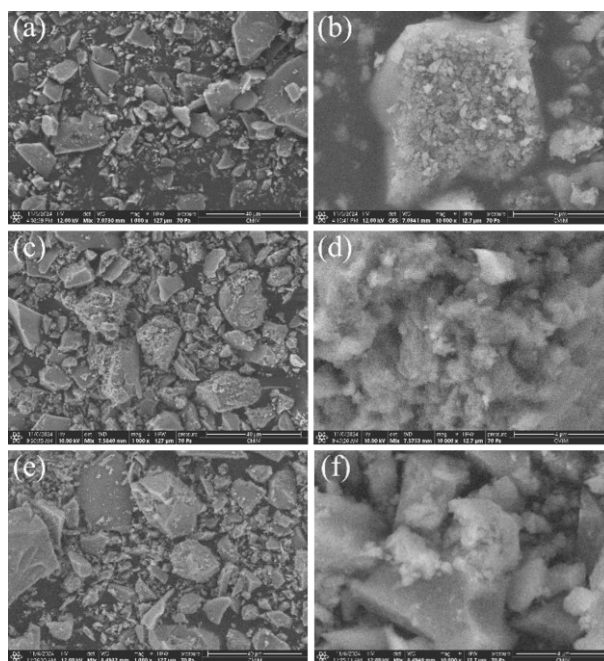


Figure 4. SEM images of (a) SiO<sub>2</sub> at 1000× and (b) 10,000× magnifications, (c) Al<sub>2</sub>O<sub>3</sub> at 1000× and (d) 10,000× magnifications, and (e) Al<sub>2</sub>O<sub>3</sub>-SiO<sub>2</sub> at 1000× and (f) 10,000× magnifications

#### 3.1.2. XRD of Synthesized Particles

The phases of the particles were analyzed by XRD. It can be indicated that all particles were amorphous (Figure 3). SiO<sub>2</sub> particle showed a diffractogram at 21.83°. The result was consistent with the research of Prasetyo *et al.* [22], who stated that the hump of amorphous SiO<sub>2</sub> is between 15° and 35°. The synthesized Al<sub>2</sub>O<sub>3</sub> particle exhibits peaks at 36.78°, 45.75°, and 67.09°, which are



assigned to the reflections of  $\gamma$ - $\text{Al}_2\text{O}_3$ . The result was in accordance with the research of Selpiana *et al.* [23], which showed peaks at  $2\theta$  angles of  $37^\circ$ ,  $46^\circ$ , and  $67^\circ$ , indicating the specific diffractogram pattern of  $\gamma$ - $\text{Al}_2\text{O}_3$ . For the  $\text{Al}_2\text{O}_3$ - $\text{SiO}_2$  particle diffractogram, two peaks were observed at  $24.78^\circ$  and  $68.10^\circ$  at low intensity. The hump at  $24.78^\circ$  is related to the amorphous  $\text{SiO}_2$ , while the low intensity diffractogram at  $68.10^\circ$  is related to  $\gamma$ - $\text{Al}_2\text{O}_3$  [22, 23].

### 3.1.3. SEM of the Synthesized Particles

The morphologies of the synthesized particles were examined using SEM. Figure 4 shows the particle images at  $1000\times$  and  $10,000\times$  magnifications. All samples exhibited irregular shapes with low uniformity. In addition, their surfaces were covered with small aggregates. These observations are consistent with the XRD results, which indicate that the particles were amorphous.

### 3.1.4. Particle Size and Polydispersity Index

The average particle sizes of the synthesized particles are presented in Figure 5, and their polydispersity indices are shown in Figure 6. Based on Figures 5 and 6, the synthesized particles are in the microscale range, with polydispersity index (PI) values  $< 1$ . Compared to the single fillers, the hybrid  $\text{Al}_2\text{O}_3$ - $\text{SiO}_2$  particles exhibit a larger particle diameter. According to Zhao *et al.* [24], the addition of additives at certain concentrations can lead to abnormal grain growth in particles. This suggests that the inclusion of  $\text{SiO}_2$  as an additive in the  $\text{Al}_2\text{O}_3$  matrix at a 1:1 ratio may promote grain growth.

Furthermore, the PI values of all formulations are below 1, indicating that the synthesized particles are homogeneously distributed. A PI value close to 0 reflects a uniform or homogeneous particle distribution, whereas a PI value close to 1 indicates a non-uniform or heterogeneous distribution [25].

### 3.1.5. FTIR of the Synthesized Particles

FTIR analysis was aimed at identifying the functional group of the synthesized particles, and their interpretations can be seen in Table 1. The  $\text{SiO}_2$  particle showed absorption peaks at  $1096$ ,  $808$ , and  $464\text{ cm}^{-1}$ , which are attributed to symmetric stretching ( $\nu_s$ ) of the siloxane ( $\text{Si-O-Si}$ ) functional group. Wavenumber at  $969\text{ cm}^{-1}$  was also observed due to the presence of  $\text{Si-OH}$  bending ( $\delta$ ) vibration. However,  $\text{SiO}_2$  particles still showed some absorptions at wavenumber  $3452$  and  $1634\text{ cm}^{-1}$ , which refer to the presence of stretching and bending hydroxyl ( $-\text{OH}$ ) vibrations, respectively [26]. An absorption of  $\text{Al}_2\text{O}_3$  particle was observed at  $809\text{ cm}^{-1}$ , which corresponds to  $\text{Al-O-Al}$  bending vibrations [27]. Nevertheless, the existence of the  $-\text{OH}$  functional group is still observed at  $3524$  and  $1629\text{ cm}^{-1}$  [28].

The FTIR spectrum of  $\text{Al}_2\text{O}_3$ - $\text{SiO}_2$  showed absorption at  $1058\text{ cm}^{-1}$ , which corresponds to asymmetric stretching ( $\nu_{as}$ ) of  $\text{Si-O-T}$  ( $T = \text{Al}$  or  $\text{Si}$ ) functional group [29]. An absorption at low intensity at  $809\text{ cm}^{-1}$  is identified as the

occurrence of  $\nu_s$   $\text{Si-O-Si}$  or  $\delta$   $\text{Al-O-Al}$  vibrations [27]. There were also wavenumbers observed at  $667$  and  $422\text{ cm}^{-1}$  that are assigned to the stretching vibrations of  $\text{Al-O}$  and  $\text{Si-O-Si}$ , respectively [26, 28]. Nonetheless, the  $-\text{OH}$  functional group is detected at wavenumber  $3458$  and  $1630\text{ cm}^{-1}$  [28].

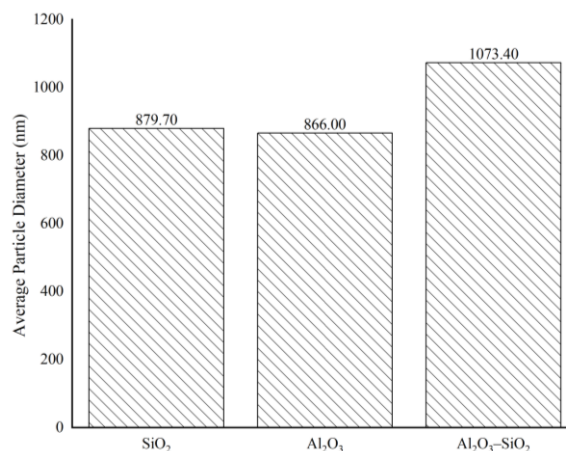


Figure 5. Particle size of  $\text{SiO}_2$ ,  $\text{Al}_2\text{O}_3$ , and  $\text{Al}_2\text{O}_3$ - $\text{SiO}_2$

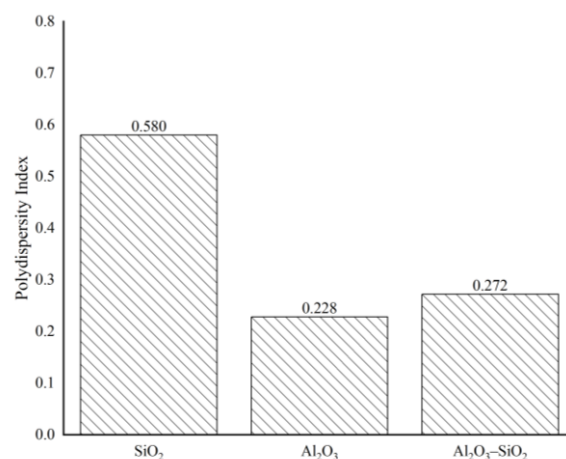


Figure 6. Polydispersity index of  $\text{SiO}_2$ ,  $\text{Al}_2\text{O}_3$ , and  $\text{Al}_2\text{O}_3$ - $\text{SiO}_2$

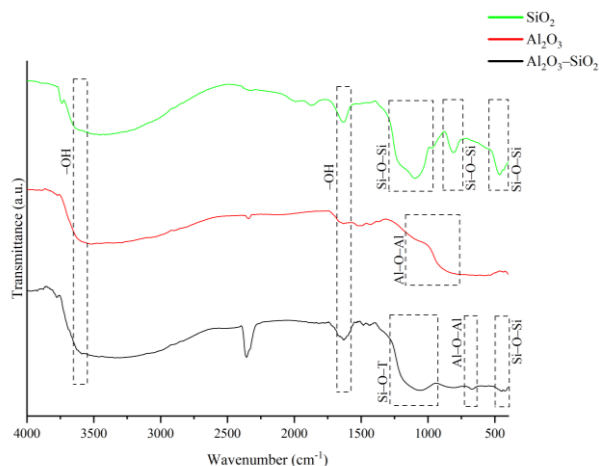
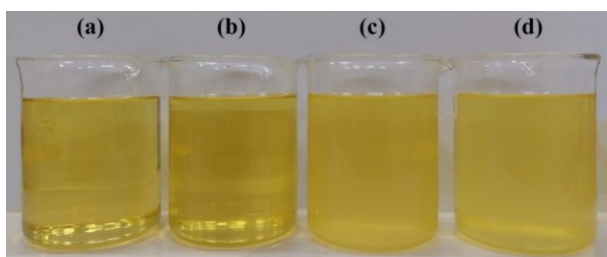


Figure 7. FTIR spectra of  $\text{SiO}_2$ ,  $\text{Al}_2\text{O}_3$ , and  $\text{Al}_2\text{O}_3$ - $\text{SiO}_2$

**Table 1.** FTIR interpretation of the synthesized particles

Compound	Wavenumber (cm <sup>-1</sup> )		Functional group
	This study	Reference	
SiO <sub>2</sub>	3452	3456 [26]	–OH symmetric and asymmetric stretching
	1634	1640 [26]	–OH symmetric bending
	1096	1101 [26]	Si–O–Si symmetric stretching
	969	950 [26]	Si–OH bending
	808	810 [26]	Si–O–Si symmetric stretching
	464	470 [26]	Si–O–Si symmetric stretching
Al <sub>2</sub> O <sub>3</sub>	3524	3427 [28]	–OH symmetric and asymmetric stretching
	1629	1636 [28]	–OH symmetric bending
	809	790 [27]	Al–O–Al bending
Al <sub>2</sub> O <sub>3</sub> –SiO <sub>2</sub>	3458	3427 [28]	–OH symmetric and asymmetric stretching
	1630	1636 [28]	–OH symmetric bending
	1058	1063 [29]	Si–O–Al or Si–O–Si asymmetric stretching
	809	790 [27]	Si–O–Si symmetric stretching or Al–O–Al bending
	667	660 [28]	Al–O stretching
	422	470 [26]	Si–O–Si symmetric stretching

**Figure 8.** Physical appearance of (a) palm oil, (b) palm oil + SiO<sub>2</sub>, (c) palm oil + Al<sub>2</sub>O<sub>3</sub>, and (d) palm oil + Al<sub>2</sub>O<sub>3</sub>–SiO<sub>2</sub>

### 3.2. Physical, Chemical, and Dielectric Properties of Synthesized Transformer Oils

#### 3.2.1. Physical Appearance of Synthesized Oils

The synthesized particles were dispersed in palm oil, sonicated for 2 hours, and heated at 105°C for 12 hours to obtain the palm-based transformer oil, as shown in Figure 8. The synthesized transformer oils were then compared based on their colors using the color scale from ASTM D1500. Overall, the dispersion of the particles did not change the colors of the synthesized transformer oils.

#### 3.2.2. Color Visualization of Synthesized Oils

Color visualization was implemented to detect the degradation of the synthesized transformer oils [30]. Color reflects the quality of the transformer oil, which can indicate the occurrence of degradation, contamination, or oxidation. In addition, the color of transformer oil becomes darker when the degradation level of the transformer increases [31]. Based on Figure 8, all the synthesized transformer oils colors were  $\leq 1$  based on the color disc, which meets the ASTM D6871-17 standard with a maximum color value of 1.

#### 3.2.3. Moisture Content of Synthesized Oils

Moisture content is a critical parameter in assessing the quality of transformer oil, as the presence of moisture can significantly affect its performance. Elevated moisture levels can increase the oil's conductivity, leading to a reduction in its breakdown voltage. This decrease in insulation performance compromises the oil's ability to withstand electrical stress, resulting in a faster occurrence of electrical breakdown [32, 33].

The presence of moisture also causes triglycerides to break down through hydrolysis into glycerol and fatty acids. The resulting fatty acids are more susceptible to oxidation compared to the stable triglycerides, impacting the quality of transformer oils. Therefore, it is crucial to minimize the moisture content of the transformer oils [34]. The moisture content analysis results of the synthesized oils were less than 200 mg/kg, which meets the ASTM D6871-17 standard. The reduction in moisture content in synthesized oils can be caused by the presence of SiO<sub>2</sub> and Al<sub>2</sub>O<sub>3</sub> particles, which have the ability to bind and absorb water in the oils [35, 36].

#### 3.2.4. Total Acid Number of Synthesized Oils

The total acid number is a crucial parameter in transformer oil, as it reflects the oil's oxidation resistance. Acidity typically arises from oxidation and secondary chemical reactions. Increased acidity negatively impacts the dielectric performance of transformer oil by raising dielectric loss and reducing BDV [37, 38]. In natural-based transformer oils, the acids formed are usually high molecular weight compounds that can increase viscosity, resulting in slower coolant flow and reduced heat transfer efficiency—factors that may compromise insulation performance and overall system efficiency [34, 37].

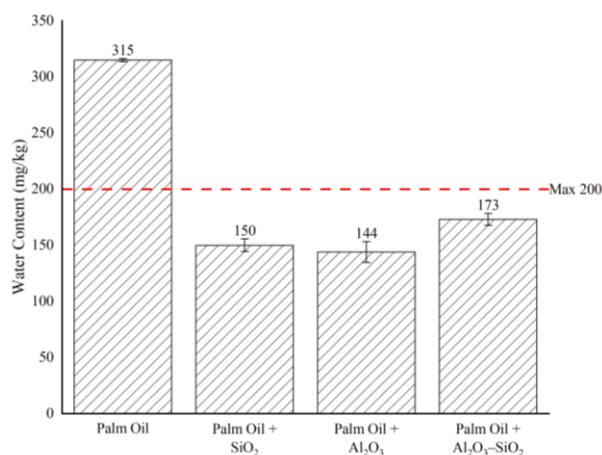


**Figure 9.** Moisture content of palm oil, palm oil + SiO<sub>2</sub>, palm oil + Al<sub>2</sub>O<sub>3</sub>, and palm oil + Al<sub>2</sub>O<sub>3</sub>-SiO<sub>2</sub>

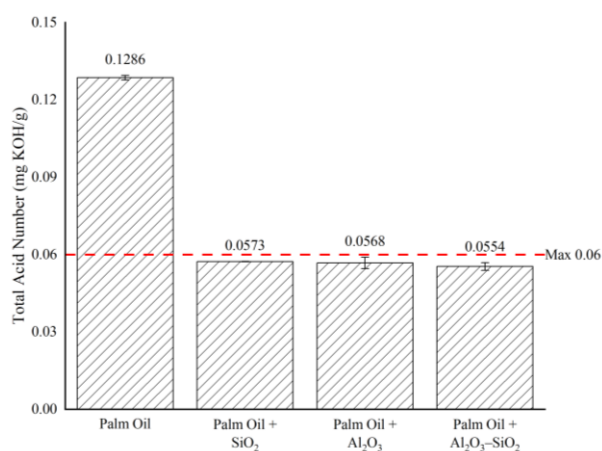


**Figure 10.** Total acid number of palm oil, palm oil + SiO<sub>2</sub>, palm oil + Al<sub>2</sub>O<sub>3</sub>, and palm oil + Al<sub>2</sub>O<sub>3</sub>-SiO<sub>2</sub>

The acid number analysis showed that all synthesized oils met the ASTM D6871-17 standard, with values below 0.06 mg KOH/g. These results may be indirectly related to the moisture content, as the particles present in the oils can mitigate the aging process by adsorbing moisture, thereby suppressing acid formation and contributing to the lower acid numbers observed [39].

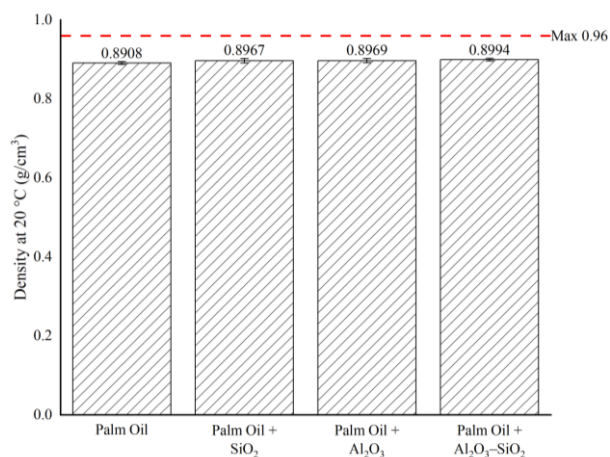


**Figure 11.** Density of palm oil, palm oil + SiO<sub>2</sub>, palm oil + Al<sub>2</sub>O<sub>3</sub>, and palm oil + Al<sub>2</sub>O<sub>3</sub>-SiO<sub>2</sub> at 20°C

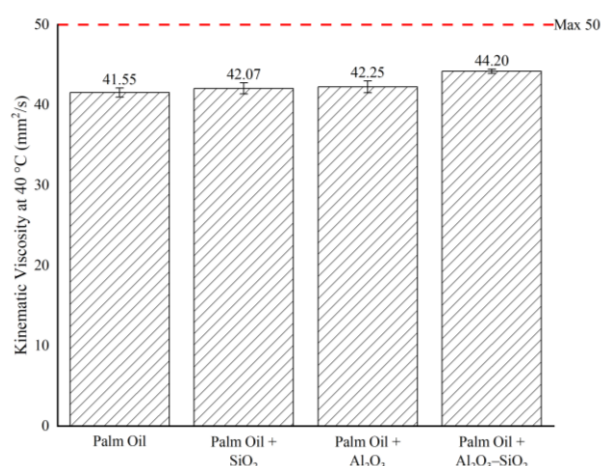


**Figure 12.** Kinematic viscosity of palm oil, palm oil + SiO<sub>2</sub>, palm oil + Al<sub>2</sub>O<sub>3</sub>, and palm oil + Al<sub>2</sub>O<sub>3</sub>-SiO<sub>2</sub> at 40°C

### 3.2.5. Density of Synthesized Oils

Although density is not the most critical parameter in determining transformer oil quality, it becomes important in lower temperature or cold climate conditions. Under such conditions, the formation of floating ice can occur, which may reduce the breakdown voltage (BDV) of the oil [12, 37]. The results of the density analysis indicated that the dispersion of particles into the oils led to an increase in their densities. Nevertheless, the densities of all synthesized oils remained within the acceptable limits defined by the ASTM D6871-17 standard.

### 3.2.6. Kinematic Viscosity of Synthesized Oils

The viscosity of transformer oil affects coolant flow and heat transfer efficiency. Higher viscosity reduces fluidity, resulting in slower coolant flow and consequently lowering the transformer's cooling performance [34, 37, 40]. Based on the results of kinematic viscosity analysis, it can be concluded that the dispersion of particles increases the kinematic viscosity of the synthesized oils. This phenomenon occurs due to the Van der Waals interactions between the particles and the oil, which restrict the molecular mobility of the oil [41]. Nevertheless, the viscosity increment of the synthesized oils still meets the standard of ASTM D6871-17 with a maximum viscosity limitation of 50 mm<sup>2</sup>/s.

### 3.2.7. BDV of Synthesized Oils

BDV reflects the maximum voltage that can be applied in the oil without forming an electric arc [42]. The efficiency of transformer oil is primarily characterized by its breakdown voltage, a critical parameter for assessing its performance under electrical stress [37]. In a base oil, the electric field is uniform, allowing electrons to accelerate and initiate a breakdown more easily. However, when fillers are present, they disrupt this uniformity by scattering the electric field lines. As a result, electrons encounter a more complex path, which reduces the occurrence of a concentrated discharge [43].

This effect leads to an increase in the number of streamer branches while also decreasing their thickness and velocity. The slower, fragmented streamers require a

higher voltage to cause complete breakdown, thereby enhancing the insulation properties of the material [43]. Based on the BDV test results, all the synthesized oils have met the IEC 62270:2018 standard, with each BDV's values over 35 kV. Additionally, Figure 14 illustrates the dielectric enhancement percentage of the synthesized transformer oils. The BDV increment of the synthesized oils was caused by the increase in trap sites originating from the dispersed particles [39]. However, compared to the single particle, the  $\text{Al}_2\text{O}_3\text{-SiO}_2$  particle shows the highest BDV improvement. The phenomenon may occur due to the synergy of the combined particles ( $\text{Al}_2\text{O}_3$  and  $\text{SiO}_2$ ), which enhances breakdown performance, leading to a higher BDV [43].

### 3.2.8. FTIR of Synthesized Oils

The FTIR spectra findings for palm oil and synthesized palm oil samples are shown in Figure 15, and the functional groups interpretation of each spectrum is shown in Table 2. The FTIR analysis of palm oil and synthesized palm oils revealed that there was no difference between any oils. Table 2 displays the spectra of the oils, with peaks at 3003, 2925, 2855, 1745, 1457, 1369, 1235, 1163, 1106, and 722  $\text{cm}^{-1}$ , respectively.

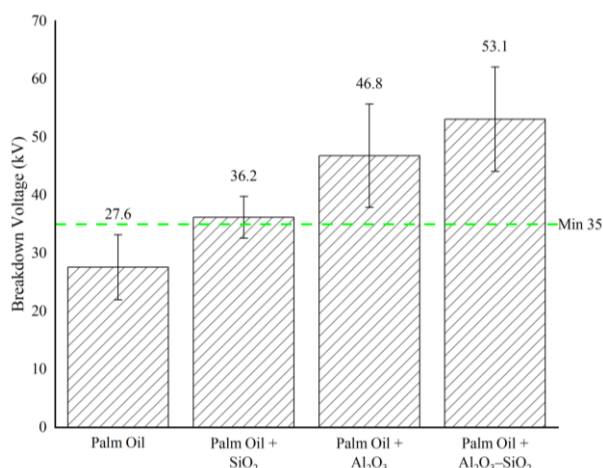


Figure 13. BDV of palm oil, palm oil +  $\text{SiO}_2$ , palm oil +  $\text{Al}_2\text{O}_3$ , and palm oil +  $\text{Al}_2\text{O}_3\text{-SiO}_2$

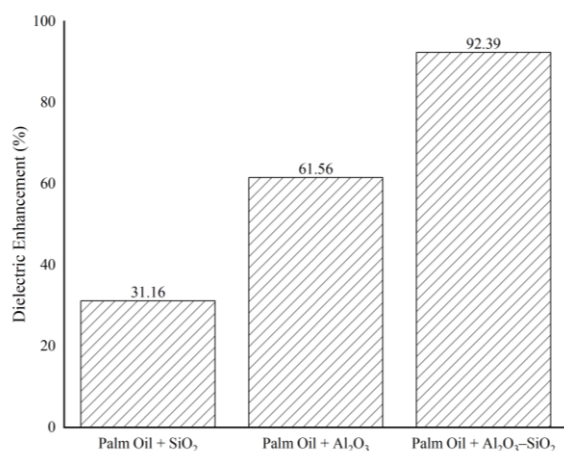


Figure 14. Dielectric enhancement of palm oil +  $\text{SiO}_2$ , palm oil +  $\text{Al}_2\text{O}_3$ , and palm oil +  $\text{Al}_2\text{O}_3\text{-SiO}_2$

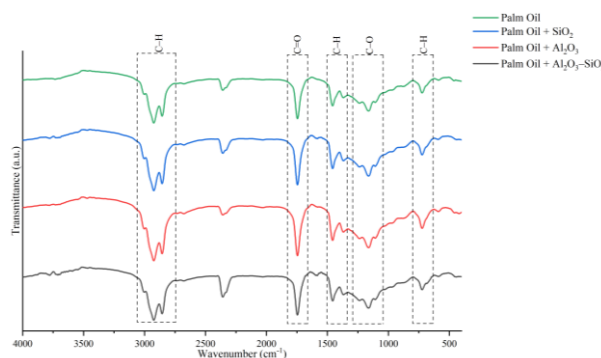


Figure 15. FTIR spectra of the synthesized transformer oils

The peak at 3003  $\text{cm}^{-1}$  represents the C–H stretching of a cis double bond ( $=\text{C-H}$ ). The peaks observed at 2925 and 2855  $\text{cm}^{-1}$  are attributed to the asymmetric and symmetric stretching vibrations of the  $\text{CH}_2$  aliphatic groups, which are characteristic of palmitic saturated fatty acids. Oleic acid may be indicated by the peak at 1745  $\text{cm}^{-1}$ , which corresponds to the stretching ( $\nu$ ) of C=O groups related to ketones or esters. The transmittance peak at 1457  $\text{cm}^{-1}$  is assigned to C–H bending, while the peak at 1369  $\text{cm}^{-1}$  corresponds to the symmetric bending ( $\delta_s$ ) vibrations of  $\text{CH}_2$  and  $\text{CH}_3$  aliphatic groups, respectively [44, 45, 46]. The wavenumber at 1233  $\text{cm}^{-1}$  is attributed to C–H bending, while the transmittance peaks at 1162 and 1106  $\text{cm}^{-1}$  correspond to the stretching vibrations of C–O ester groups. Finally, the peak at 722  $\text{cm}^{-1}$  indicates cis C–H out-of-plane bending vibrations [45, 46, 47, 48].

Overall, the addition of fillers to the palm-based transformer oils did not introduce new absorption bands or cause noticeable peak shifts, indicating that the fillers do not significantly alter the chemical structure of the oils. Similar findings were reported by Mohamad *et al.* [49], who detected no observable shifts in palm oil after the addition of  $\text{Al}_2\text{O}_3$  particles.

Table 2. Functional groups interpretation of palm oil and synthesized palm oils

Wavenumber ( $\text{cm}^{-1}$ )		
Palm oil and synthesized palm oils	Reference	Functional group
3003	3012 [44]	C–H stretching
2925	2922–2921 [45]	C–H asymmetric stretching
2855	2853–2852 [45]	C–H symmetric stretching
1745	1743–1742 [45]	C=O stretching
1457	1461 [46]	C–H bending
1369	1377 [44]	C–H symmetric bending
1233	1400–1200 [47]	C–H bending
1162	1160 [46]	C–O stretching
1106	1111 [45]	C–O stretching
722	715 [48]	C–H bending out of plane



#### 4. Conclusion

$\text{Al}_2\text{O}_3\text{-SiO}_2$  was successfully synthesized using the sol-gel method. Characterization results confirmed that the synthesized fillers were micro-sized and exhibited an amorphous phase. The particles were dispersed into palm oils and analyzed for their physicochemical and dielectric properties. Based on visual observation, particle dispersion did not alter the color of the synthesized oils. FTIR analysis also confirmed that the dispersion of particles did not modify the chemical structure of the palm-based transformer oils. Overall, all synthesized oils met the requirements of ASTM D6871-17 and IEC 62270:2018. Compared to the single filler, the hybrid  $\text{Al}_2\text{O}_3\text{-SiO}_2$  dispersed in palm-based transformer oil produced more notable improvements, particularly in dielectric properties. This finding suggests that hybrid  $\text{Al}_2\text{O}_3\text{-SiO}_2$  offers superior physicochemical and dielectric performance as a filler for palm-based transformer oil. Furthermore, the results indicate the potential application of hybrid  $\text{Al}_2\text{O}_3\text{-SiO}_2$  in improving the dielectric properties of natural-based transformer oils.

#### References

- [1] Stephanie Azlyn Anak Felix, Muhamad Faiz Md Din, Asnor Mazuan Ishak, Jianli Wang, Nurul Hayati Idris, Wan Fathul Hakim Wan Zamri, Investigation of the Electrical Properties of Mineral Oils with and without Carbon Nanotube Concentration under Different Magnetic Fields Applied in Transformer Applications, *Energies*, 16, 8, (2023), 3381 <https://doi.org/10.3390/en16083381>
- [2] Hesham S. Karaman, Daa-Eldin A. Mansour, Matti Lehtonen, Mohamed M. F. Darwish, Condition Assessment of Natural Ester-Mineral Oil Mixture Due to Transformer Retrofilling via Sensing Dielectric Properties, *Sensors*, 23, 14, (2023), 6440 <https://doi.org/10.3390/s23146440>
- [3] Konstantinos N. Koutras, Ioannis A. Naxakis, Aspasia E. Antonelou, Vasilios P. Charalampakos, Eleftheria C. Pyrgioti, Spyros N. Yannopoulos, Dielectric strength and stability of natural ester oil based  $\text{TiO}_2$  nanofluids, *Journal of Molecular Liquids*, 316, (2020), 113901 <https://doi.org/10.1016/j.molliq.2020.113901>
- [4] Muhammad Rafiq, Muhammad Shafique, Anam Azam, Muhammad Ateeq, Israr Ahmad Khan, Abid Hussain, Sustainable, Renewable and Environmental-Friendly Insulation Systems for High Voltages Applications, *Molecules*, 25, 17, (2020), 3901 <https://doi.org/10.3390/molecules25173901>
- [5] Zaid B. Siddique, Soumen Basu, Prasenjit Basak, Dielectric behavior of natural ester based mineral oil blend dispersed with  $\text{TiO}_2$  and  $\text{ZnO}$  nanoparticles as insulating fluid for transformers, *Journal of Molecular Liquids*, 339, (2021), 116825 <https://doi.org/10.1016/j.molliq.2021.116825>
- [6] Siti Sarah Junian, Mohamad Zul Hilmey Makmud, Zuhair Jamain, Khairatun Najwa Mohd Amin, Jedol Dayou, Hazlee Azil Illias, Effect of Rice Husk Filler on the Structural and Dielectric Properties of Palm Oil as an Electrical Insulation Material, *Energies*, 14, 16, (2021), 4921 <https://doi.org/10.3390/en14164921>
- [7] Mohd Safwan Mohamad, Hidayat Zainuddin, Sharin Ab Ghani, Imran Sutan Chairul, AC breakdown voltage and viscosity of palm fatty acid ester (PFAE) oil-based nanofluids, *Journal of Electrical Engineering and Technology*, 12, 6, (2017), 2333-2341 <https://doi.org/10.5370/JEET.2017.12.6.2333>
- [8] Wittawat Saenkhumwong, Amnart Suksri, The improved dielectric properties of natural ester oil by using  $\text{ZnO}$  and  $\text{TiO}_2$  nanoparticles, *Engineering and Applied Science Research*, 44, 3, (2017), 148-153 <https://doi.org/10.14456/easr.2017.22>
- [9] Usama Khaled, Abderrahmane Beroual, Influence of Conductive Nanoparticles on the Breakdown Voltage of Mineral Oil, Synthetic and Natural Ester Oil-based Nanofluids, 2019 IEEE 20th International Conference on Dielectric Liquids (ICDL), Roma, Italy, 2019 <https://doi.org/10.1109/ICDL.2019.8796530>
- [10] Khoirudin Khoirudin, Budi Kristiawan, Budi Santoso, Sukarman Sukarman, Amri Abdullah, Heat Transfer Characteristic of  $\text{Al}_2\text{O}_3$  Nanofluid with Naphthenic Transformers Oil as Base Fluid, *Journal of Advanced Research in Fluid Mechanics and Thermal Sciences*, 128, 2, (2025), 86-97 <https://doi.org/10.37934/arfmts.128.2.8697>
- [11] Jorge Martins, Asal Kiazadeh, Joana V. Pinto, Ana Rovisco, Tiago Gonçalves, Jonas Deuermeier, Eduardo Alves, Rodrigo Martins, Elvira Fortunato, Pedro Barquinha,  $\text{Ta}_2\text{O}_5/\text{SiO}_2$  Multicomponent Dielectrics for Amorphous Oxide TFTs, *Journal of Electronic Materials*, 2, 1, (2021), 1-16 <https://doi.org/10.3390/electronicmat2010001>
- [12] Xiaobo Wang, Chao Tang, Bo Huang, Jian Hao, George Chen, Review of Research Progress on the Electrical Properties and Modification of Mineral Insulating Oils Used in Power Transformers, *Energies*, 11, 3, (2018), 487 <https://doi.org/10.3390/en11030487>
- [13] Maryam Khosravi Mardkhe, Baiyu Huang, Calvin H. Bartholomew, Todd M. Alam, Brian F. Woodfield, Synthesis and characterization of silica doped alumina catalyst support with superior thermal stability and unique pore properties, *Journal of Porous Materials*, 23, 2, (2016), 475-487 <https://doi.org/10.1007/s10934-015-0101-z>
- [14] Yu Wu, Xiaodong Wang, Lin Liu, Ze Zhang, Jun Shen, Alumina-Doped Silica Aerogels for High-Temperature Thermal Insulation, *Gels*, 7, 3, (2021), 122 <https://doi.org/10.3390/gels7030122>
- [15] Yulin Tian, Xiaodong Wang, Yu Wu, Xiaoxue Zhang, Chun Li, Yijun Wang, Jun Shen, A Facile Method to Fabricate  $\text{Al}_2\text{O}_3\text{-SiO}_2$  Aerogels with Low Shrinkage up to 1200°C, *Molecules*, 28, 6, (2023), 2743 <https://doi.org/10.3390/molecules28062743>
- [16] N. K. Deenesh, A. Mahmood, Ghazali Kadir, Khalid Hasnan, N. Nafarizal, Experimental investigation on thermal conductivity and viscosity of purified aged transformer oil based  $\text{SiO}_2$ ,  $\text{Al}_2\text{O}_3$  and  $\text{TiO}_2$  nanofluid for Electric Multiple Unit Train, *Journal of Physics: Conference Series*, 1878, (2021), 012017 <https://doi.org/10.1088/1742-6596/1878/1/012017>
- [17] Raymon Antony Raj, Ravi Samikannu, Abid Yahya, Modisa Mosalaosi, Investigation of Survival/Hazard Rate of Natural Ester Treated with  $\text{Al}_2\text{O}_3$  Nanoparticle for Power Transformer Liquid



- Dielectric, *Energies*, 14, 5, (2021), 1510  
<https://doi.org/10.3390/en14051510>
- [18] S. Razak, M. R. M. Naw, M. Z. A. Rehim, W. H. Azmi, Preparation Technique of SiO<sub>2</sub>/HFE 7000 Nanorefrigerant, *Journal of Mechanical Engineering*, SI 5, 5, (2018), 132–140
- [19] A. A. M. Redhwan, W. H. Azmi, M. Z. Sharif, N. N. M. Zawawi, R. Mamat, Sonication time effect towards stability of Al<sub>2</sub>O<sub>3</sub>/PAG and SiO<sub>2</sub>/PAG nanolubricants, *Journal of Mechanical Engineering*, 5, 1, (2018), 14–27
- [20] Md Rizwan, Suhaib Ahmad Khan, M. Rizwan Khan, Asfar Ali Khan, Experimental and statistical investigation on the dielectric breakdown of magneto nanofluids for power applications, *Journal of Materials Science: Materials in Engineering*, 19, 1, (2024), 5 <https://doi.org/10.1186/s40712-024-00144-0>
- [21] Bela Amelia, Amnur Akhyan, Experimental Study of the Effect of Crude Palm Oil (Non-Newtonian Fluid) Viscosity on Increasing Flowrate Capacity, *Proceeding International The 10<sup>th</sup> Applied Business and Engineering Conference 2022*, 2023
- [22] A. B. Prasetyo, M. Handayani, E. Sulistiyono, A. N. Syahid, E. Febriana, W. Mayangsari, E. Y. Muslih, F. Nugroho, F. Firdiyono, Development of high purity amorphous silica from emulsifier silicon by pyrolysis process at temperature of 700°C, *Journal of Physics: Conference Series*, 2190, 1, (2022), 012013 <https://doi.org/10.1088/1742-6596/2190/1/012013>
- [23] Selpiana Selpiana, David Bahrin, R. R. Yunita Bayu Ningsih, Aditia H. Akbar, Ayu Permatasari, Synthesis and Characterization Catalyst  $\gamma$ -Al<sub>2</sub>O<sub>3</sub> and Al/ $\gamma$ -Al<sub>2</sub>O<sub>3</sub> Using XRD Analysis, *Indonesian Journal of Fundamental and Applied Chemistry*, 7, 1, (2022), 26–31 <http://dx.doi.org/10.24845/ijfac.v7.i1.26>
- [24] Quanbao Zhao, Zhihong Li, Yumei Zhu, Effect of CaO-TiO<sub>2</sub>-SiO<sub>2</sub> on the Microstructure and Mechanical Properties of Ceramic Corundum Abrasives, *Inorganics*, 11, 5, (2023), 187 <https://doi.org/10.3390/inorganics11050187>
- [25] Dian Eka Ermawati, Samrotul Jannah, The Effect of Surfactant Concentration to Particle Size and Loading Dose of Immunity Jamu's Ethanolic Extract SNEDDS (Self-Nano Emulsifying Drugs Delivery System), *Majalah Obat Tradisional*, 28, 2, (2023), 102–111 <https://doi.org/10.22146/mot.83321>
- [26] Asmaa Mourhly, Mariam Khachani, Adnane El Hamidi, Mohammed Kacimi, Mohammed Halim, Said Aarsalane, The Synthesis and Characterization of Low-Cost Mesoporous Silica SiO<sub>2</sub> from Local Pumice Rock, *Nanomaterials and Nanotechnology*, 5, (2015), 35 <https://doi.org/10.5772/62033>
- [27] Xiangtao Lin, Zhikai Wang, Xingxing Jiang, Tianxiang Ning, Yong Jiang, Anxian Lu, Effect of Al<sub>2</sub>O<sub>3</sub>/SiO<sub>2</sub> mass ratio on the structure and properties of medical neutral boroaluminosilicate glass based on XPS and infrared analysis, *Ceramics International*, 49, 23, Part B, (2023), 38499–38508 <https://doi.org/10.1016/j.ceramint.2023.09.180>
- [28] Izabela Rutkowska, Jakub Marchewka, Piotr Jeleń, Mateusz Odziomek, Mateusz Korpyś, Joanna Paczkowska, Maciej Sitarz, Chemical and Structural Characterization of Amorphous and Crystalline Alumina Obtained by Alternative Sol–Gel Preparation Routes, *Materials*, 14, 7, (2021), 1761 <https://doi.org/10.3390/ma14071761>
- [29] Sujitra Onutai, Takeshi Osugi, Tomoyuki Sone, Alumino-Silicate Structural Formation during Alkali-Activation of Metakaolin: In-Situ and Ex-Situ ATR-FTIR Studies, *Materials*, 16, 3, (2023), 985 <https://doi.org/10.3390/ma16030985>
- [30] Hussain Kalathiripi, Subrata Karmakar, Analysis of transformer oil degradation due to thermal stress using optical spectroscopic techniques, *International Transactions on Electrical Energy Systems*, 27, 9, (2017), e2346 <https://doi.org/10.1002/etep.2346>
- [31] Janvier Sylvestre N'cho, Issouf Fofana, Yazid Hadjadj, Abderrahmane Beroual, Review of Physicochemical-Based Diagnostic Techniques for Assessing Insulation Condition in Aged Transformers, *Energies*, 9, 5, (2016), 367 <https://doi.org/10.3390/en9050367>
- [32] Sharin Ab Ghani, Norazhar Abu Bakar, Imran Sutan Chairul, Mohd Shahril Ahmad Khair, Nur Hakimah Ab Aziz, Effects of Moisture Content and Temperature on the Dielectric Strength of Transformer Insulating Oil, *Journal of Advanced Research in Fluid Mechanics and Thermal Sciences*, 63, 1, (2024), 107–116
- [33] Muhamad Mustangin, Bambang Purwantana, Chusnul Hidayat, Radi, Development of high free fatty acid crude palm oil as a biodegradable electrical liquid insulator as an alternative to mineral oil-based insulators, *Cleaner Engineering and Technology*, 18, (2024), 100712 <https://doi.org/10.1016/j.clet.2023.100712>
- [34] Esther Ogwa Obebe, Yazid Hadjadj, Samson Okikiola Oparanti, Issouf Fofana, Enhancing the Performance of Natural Ester Insulating Liquids in Power Transformers: A Comprehensive Review on Antioxidant Additives for Improved Oxidation Stability, *Energies*, 18, 7, (2025), 1690 <https://doi.org/10.3390/en18071690>
- [35] Wenxin Tian, Chao Tang, Qian Wang, Shiling Zhang, Yali Yang, The Effect and Associate Mechanism of Nano SiO<sub>2</sub> Particles on the Diffusion Behavior of Water in Insulating Oil, *Materials*, 11, 12, (2018), 2373 <https://doi.org/10.3390/ma11122373>
- [36] Rui Chen, Zhongyong Zhao, Ziming Su, Dong Huang, Chao Tang, Effect of nano-Al<sub>2</sub>O<sub>3</sub> on water molecular diffusion in natural ester: A molecular dynamics simulation, *Journal of Molecular Liquids*, 375, (2023), 121326 <https://doi.org/10.1016/j.molliq.2023.121326>
- [37] Sandra Sorte, Alexandre Salgado, André Ferreira Monteiro, Diogo Ventura, Nelson Martins, Mónica S. A. Oliveira, Advancing Power Transformer Cooling: The Role of Fluids and Nanofluids—A Comprehensive Review, *Materials*, 18, 5, (2025), 923 <https://doi.org/10.3390/ma18050923>
- [38] Samson Okikiola Oparanti, Ungarala Mohan Rao, Issouf Fofana, Natural Esters for Green Transformers: Challenges and Keys for Improved Serviceability, *Energies*, 16, 1, (2023), 61 <https://doi.org/10.3390/en16010061>
- [39] Rizwan A. Farade, Noor Izzri Abdul Wahab, Muhammad Rafiq, Nehad Ali Shah, T. M. Yunus Khan, Syed Waheedullah Ghor, Cutting-edge dielectric nanofluids: a review of factors influencing stability and thermo-dielectric properties, *Journal of*

*Thermal Analysis and Calorimetry*, (2025),  
<https://doi.org/10.1007/s10973-025-14631-9>

breakdown voltage of palm oil and coconut oil based  $\text{Al}_2\text{O}_3$  nanofluids, *Nanotechnology*, 31, 42, (2020), 425708 <https://doi.org/10.1088/1361-6528/aba1b9>

- [40] Muhammad Nazori Deraman, Norazhar Abu Bakar, Nur Hakimah Ab Aziz, Imran Sutan Chairul, The experimental study on the potential of waste cooking oil as a new transformer insulating oil, *Journal of Advanced Research in Fluid Mechanics and Thermal Sciences*, 69, 1, (2020), 74-84  
<https://doi.org/10.37934/arfm.69.1.7484>
- [41] Charishma Almeida, Sohan Paul, Lazarus Godson Asirvatham, Stephen Manova, Rajesh Nimmagadda, Jefferson Raja Bose, Somchai Wongwises, Experimental Studies on Thermophysical and Electrical Properties of Graphene-Transformer Oil Nanofluid, *Fluids*, 5, 4, (2020), 172  
<https://doi.org/10.3390/fluids5040172>
- [42] Mahmood Ali, N. K. Deenesh, Ghazali Kadir, Khalid Hasnan, Nafarizal Nayan, Effect of purification process on the thermal conductivity and breakdown voltage of inhibited, isoparaffinic transformer oil used in electric train, *Journal of Physics: Conference Series*, 1878, (2021), 012009  
<https://doi.org/10.1088/1742-6596/1878/1/012009>
- [43] Rizwan A. Farade, Noor Izzri Abdul Wahab, Diao-Eldin A. Mansour, Muhammad Rafiq, T. M. Yunus Khan, Abdul Saddique Shaik, Maciej Zdanowski, Sharanabasava V. Ganachari, Reji Kumar Rajamony, Ramjan Ahamad Khatik, Abdul Nazeer, Dielectric Nanofluids for Transformers: A Review on Stability, Dielectric, Thermophysical, and Chemical Properties, *IEEE Access*, 13, (2025), 142467-142492  
<https://doi.org/10.1109/ACCESS.2025.3597740>
- [44] Ng Jing Sheng, Widad Fadhullah, Mohd Omar Ab Kadir, Ainolsyakira Mohd Rodhi, Noor Hana Hanif Abu Bakar, Syahidah Akmal Muhammad, An assessment of FT-IR and FT-NIR capability in screening crude palm oil authenticity and quality combined with chemometrics, *Malaysian Journal of Analytical Sciences*, 23, 5, (2019), 870-879
- [45] Pichai Muangpratoom, Chinnapat Suriyasakulpong, Sakda Maneerot, Wanwilai Vittayakorn, Norasage Pattanadech, Experimental Study of the Electrical and Physiochemical Properties of Different Types of Crude Palm Oils as Dielectric Insulating Fluids in Transformers, *Sustainability*, 15, 19, (2023), 14269  
<https://doi.org/10.3390/su151914269>
- [46] Zanariah Hashim, S. S. A. Zaki, Mad, Ida Idayu Muhamad, Quality assessment of fried palm oils using fourier transform infrared spectroscopy and multivariate approach, *Chemical Engineering Transactions*, 56, (2017), 829-834  
<https://doi.org/10.3303/CET1756139>
- [47] A. G. Jacob, I. Musa, A. B. Ogbesejana, Extraction, FTIR and GC-MS characterization of palm kernel oil for laundry soap production, *Scientia Africana*, 23, 3, (2024), 185-196 <https://doi.org/10.4314/sa.v23i3.18>
- [48] A. Windarsih, Irnawati, A. Rohman, The use of FTIR spectroscopy in combination with chemometrics for the authentication of milk fat from palm oil, *IOP Conference Series: Materials Science and Engineering*, 980, 1, (2020), 012025 <https://doi.org/10.1088/1757-899X/980/1/012025>
- [49] Nur Aqilah Mohamad, Norhafiz Azis, Jasronita Jasni, Mohd Zainal Abidin Ab. Kadir, Robiah Yunus, Zaini Yaakub, Effect of surfactants on the lightning